Fast stereoselective reactions in electrosprayed Co(II)/neurotransmitter nanodroplets†

Caterina Fraschetti,[a] Massimiliano Aschi,[b] Antonello Filippi,[a] Anna Giardini[c] and Maurizio Speranza*[a]

Received (in Cambridge, UK) 22nd January 2008, Accepted 5th March 2008
First published as an Advance Article on the web 4th April 2008
DOI: 10.1039/b801201f

Collision induced dissociation (CID) of the *m/z* 479 ion, formed by ESI of $Co(NO_3)_2$–CH_3OH solutions with either pure (1*S*,2*S*)-(+)-*N*-methylpseudoephedrine or its mixtures with (1*S*,2*R*)-(+)- or (1*R*,2*S*)-(−)-ephedrine, provides compelling evidence for fast, stereoselective reactions in Co(II)/neurotrasmitter(s) aggregates during solvent evaporation of the ESI droplets.

Electrospray ionization (ESI) has become a well integrated tool for mass spectrometry (MS) because of its capability to put in the gas phase a variety of non-volatile analytes, such as peptides,[1,2] proteins,[3–6] drugs,[7] polymers,[8] organometallics,[9,10] inorganics,[9,11] and even viruses[12,13] and bacteria,[14] as well as noncovalent supramolecular aggregates.[15–18] However, the processes and mechanisms that must occur for production of these gas-phase species from bulk solutions are inadequately understood.[19,20] The problem arises from the intrinsic difficulties in observing the formation and the behaviour of submicron charged droplets from solution and, more importantly, how the concentration and the distribution of the analytes in these droplets change during the time evolution of the electrospray plume.

In ESI, the charge on the analyte is either already present, such as for inorganic salts, or induced by charge deposition to the droplet containing a neutral analyte, *e.g.* an organic compound. Therefore, it is not surprising that the ionization efficiency and the ESI-MS spectrum of a solution are strongly influenced by the nature and the concentration of the solutes. Indeed, it may happen that the relative abundance of the ionic species from ESI does not reproduce at all the distribution of the analytes at equilibrium in solutions.[20–23] However, it would be quite surprising to verify that the chemical nature itself of the ionic species from ESI is different from that of their stable precursors in solutions. In other words, the question arises as to whether and to what extent stable analytes at equilibrium in solutions do undergo chemical transformations during the time evolution of the electrospray nanodroplet. Since ESI-MS is commonly qualified as a reliable analytical tool, answering this question would be right and proper.

In the course of a comprehensive ESI-MS investigation on the structure and the relative stability of noncovalent diastereomeric Co(II) complexes with the neurotransmitters of Table 1, we noticed that their collision induced fragmentation (CID) not only reflected the expected connectivity of the relevant noncovalent complexes, but also that of other isomeric structures. More importantly, their relative abundance was found to be strongly dependent on the presence, the nature, the configuration, and the concentration of other components present in the electrosprayed solution. On the grounds of these observations, we will provide in this paper clear-cut evidence in favor of the party supporting ESI droplets as potential nanoreactors.

The ESI-MS-CID experiments were performed on a Applied Biosystems Linear Ion Trap API 2000 mass spectrometer equipped with an electrospray ionization (ESI) source and a syringe pump.‡ Either pure (1*S*,2*S*)-(+)-*N*-methylpseudoephedrine ($^{(+)}$**M**) or its mixtures with either (1*S*,2*R*)-(+)-ephedrine ($^{(+)}$**E**) or (1*R*,2*S*)-(−)-ephedrine ($^{(-)}$**E**), or their hydrochlorides ($^{(+)}$**E**·HCl or $^{(-)}$**E**·HCl), were added to methanolic solutions of $Co(NO_3)_2$ (1×10^{-4} M). The overall concentration of the neurotrasmitter(s) was 4×10^{-4} M. ESI of these mixtures leads to complex ion patterns wherefrom a sufficiently intense *m/z* 479 peak can be detected which would nominally correspond to the $[(^{(+)}M)_2CoNO_3]^+$ aggregate. After its isolation from the accompanying ions in the first quadrupole of the instrument, the *m/z* 479 ion was allowed to collide in the second RF-only quadrupole with N_2 molecules and to fragment (CID). A reproducible ion fragmentation pattern was observed, characterized by fragments at: (i) *m/z* 416 (by formal loss of HNO_3); (ii) *m/z* 403 (by formal loss of CH_2ONO_2); (iii) *m/z* 402 (by formal loss of CH_3ONO_2); (iv) *m/z* 180 (MH^+); and (v) *m/z* 166 (EH^+). Fragments (i)–(iii)

Table 1 Structures and symbols of the employed neurotransmitters

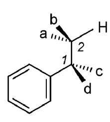

a	b	c	d	Symbol
$N(CH_3)_2$	CH_3	H	OH	$^{(+)}$**M**
CH_3	$NHCH_3$	H	OH	$^{(+)}$**E**
$NHCH_3$	CH_3	OH	H	$^{(-)}$**E**
CH_3	$NH_2CH_3{}^+Cl^-$	H	OH	$^{(+)}$**E**·HCl
$NH_2CH_3{}^+Cl^-$	CH_3	OH	H	$^{(-)}$**E**·HCl

[a] *Dipartimento di Studi di Chimica e Tecnologia delle Sostanze Biologicamente Attive, Università di Roma "La Sapienza", Rome, Italy. E-mail: maurizio.speranza@uniroma1.it; Fax: +39-06-49913497; Tel: +39-06-49913602*
[b] *Dipartimento di Chimica, Ingegneria Chimica e Materiali, Università degli Studi di L'Aquila, L'Aquila, Italy*
[c] *CNR IMIP, Italy*

† Electronic supplementary information (ESI) available: HPLC-MS chromatograms of **E**–**M**–$Co(NO_3)_2$ solutions; some CID spectra of the *m/z* 479 ion from ESI of **E**–**M**–$Co(NO_3)_2$ and **M**–$Co(NO_3)_2$ solutions. See DOI: 10.1039/b801201f

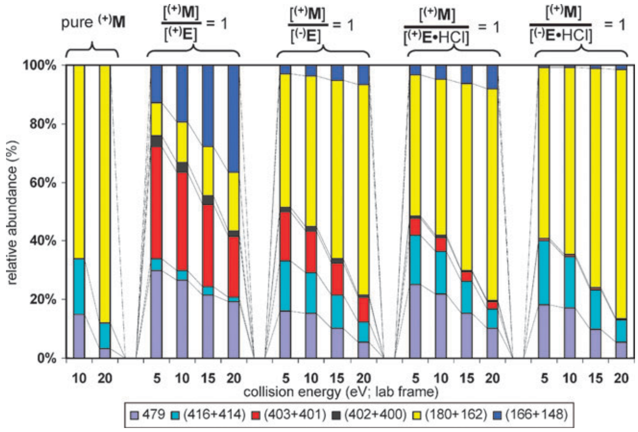

Fig. 1 Relative abundance of the fragment ions from CID of m/z 479 from pure **M** and [**M**]/[**E**] = 1 solutions as a function of the collision energy (E_{lab}).

are accompanied by their dehydrogenated forms, *i.e.* m/z 414, 401 and 400, respectively, whereas fragments (iv) and (v) by their dehydrated forms, *i.e.* m/z 162 and 148, respectively. The pair of fragments differing for the loss of a hydrogen or a water molecule will be henceforth denoted by writing in italic the mass of the parent fragment, *e.g.* m/z *416* for m/z 416 + m/z 414 and m/z *180* for m/z 180 + m/z 162. The neutral species accompanying their formation will also be denoted in italic (*e.g.* HNO_3 for the loss of HNO_3 (to give m/z 416) and of HNO_3 + H_2 (to give m/z 414 from m/z 479)).

The combined relative abundances of each pair of fragments are given in Fig. 1 and 2 together with the composition of the relevant mixtures. Fig. 1 shows that the ion pattern from CID of m/z 479 dramatically depends on the presence of ephedrine **E** in the **M**–$Co(NO_3)_2$–CH_3OH mixtures (*cf. e.g.* pure $^{(+)}$**M** and [$^{(+)}$**M**]/[$^{(+)}$**E**] = 1). CID of m/z 479, formed from the pure $^{(+)}$**M** solutions, leads exclusively to m/z *416* (by loss of HNO_3) and to m/z *180* (by formal loss of *(**M** − H)CoNO₃*). As evident from Fig. 1, the latter fragmentation is more energy demanding than the first one. This ion pattern is suggestive of structures for m/z 479 where **M** is the only organic species coordinated to Co(II), *i.e.* $[\mathbf{M}_2CoNO_3]^+$ and its $[(\mathbf{M}-H)\mathbf{M}CoNO_3H]^+$ protomer. The latter ion may be responsible of the formation of m/z *416* (*[(**M** − H)**M**Co]$^+$*), while both may account for the formation of the m/z *180* (***MH***$^+$). In contrast, CID of m/z 479, formed from the solutions with variable concentrations of **E** (Fig. 2) yields, besides m/z *416* and m/z *180*, sizable amounts of m/z *403* (by formal loss of CH_2ONO_2), m/z *402* (by formal loss of CH_3ONO_2), and ***EH***$^+$ (m/z *166*; by formal loss of *(**M** − H)CoCH₂ONO₂)* as well (see Electronic Supplementary Information†). Such an unexpected result is indicative of the occurrence of several isomers of $[\mathbf{M}_2CoNO_3]^+$ and $[(\mathbf{M}-H)\mathbf{M}CoNO_3H]^+$ wherein one **M** ligand has been replaced by an **E** molecule, *i.e.* $[\mathbf{ME}CoCH_2ONO_2]^+$ and $[(\mathbf{M}-H)\mathbf{E}CoCH_3ONO_2]^+$. Indeed, the latter ion may be responsible for the formation of m/z *402* (*[(**M** − H)**E**Co]$^+$*) by formal loss of CH_3ONO_2 and the first one of the formation of the m/z *403* (*[**ME**Co]$^+$*) by formal loss of CH_2ONO_2. Furthermore, both ions may account for the more energy demanding formation of the of ***EH***$^+$ fragment. Since careful HPLC-MS analysis of all the ESI-MS analyzed **M**–**E**–$Co(NO_3)_2$–CH_3OH mixtures did not show any detectable time-dependent chemical modification even after *ca.* 1 month (see Electronic Supplementary Information†), the results of Fig. 1 are consistent with fast reactions of ephedrine with the precursor(s) of the m/z 479 species occurring by the time of ESI droplets evaporation. This view is supported by the observation that the ionic patterns from CID of m/z 479 is strongly sensitive to: (i) the specific form of ephedrine, whether as a neutral molecule or as the hydrochloride salt (*cf. e.g.* $^{(+)}$**M**/$^{(+)}$**E** and $^{(+)}$**M**/$^{(+)}$**E**·HCl; Fig. 1); (ii) the [**M**]/[**E**] concentration ratio (a–c in Fig. 2); and (iii) the specific configuration of ephedrine (*cf. e.g.* $^{(+)}$**M**/$^{(+)}$**E** and $^{(+)}$**M**/$^{(-)}$**E**; Fig. 1).

In particular, formation of the $[\mathbf{ME}CoCH_2ONO_2]^+$ and $[(\mathbf{M}-H)\mathbf{E}CoCH_3ONO_2]^+$ isomers is depressed when ephedrine is in the hydrochloride form (red and black bars of Fig. 1) and at the lowest ephedrine concentrations (red and black bars of Fig. 2). This latter effect is particularly pronounced with the $^{(-)}$**E** or $^{(-)}$**E**·HCl enantiomers, whereas it is less evident with the $^{(+)}$**E** or $^{(+)}$**E**·HCl ones (Fig. 2).

In the presence of $^{(-)}$**E** or $^{(-)}$**E**·HCl, the relative abundance of m/z *416* increases by increasing the [**M**]/[**E**] ratio (a → c in Fig. 2), whereas the reverse is true for the m/z *403* and m/z *402* fragments. This opposite behavior can be accounted for by fast **E** ⇆ **M** ligand exchange in the ESI-formed precursors of the m/z 479 ion. At the highest [**E**] (a in Fig. 2), the **E** → **M** displacement is favoured over the reverse **E** ← **M** one. As illustrated in Scheme 1, this enhances the contribution of the $[\mathbf{ME}CoCH_2ONO_2]^+$ and $[(\mathbf{M}-H)\mathbf{E}CoCH_3ONO_2]^+$ isomeric structures to the m/z 479 signal at the expense of the $[\mathbf{M}_2CoNO_3]^+$ and $[(\mathbf{M}-H)\mathbf{M}CoNO_3H]^+$ ones. The consequence is a decrease of the m/z 479 → m/z *416*; m/z *180* fragmentation channels and a parallel increase of the m/z 479 → m/z *403*; m/z *402*; m/z *166* ones. At the highest [**M**] (c in Fig. 2), the **M** → **E** displacement is favoured and the opposite trend is observed. The fact that these effects are much less evident in the presence of $^{(+)}$**E** or $^{(+)}$**E**·HCl components denotes a marked stereoselectivity of the **E** ⇆ **M** ligand exchange in the precursors of the m/z 479 ion.

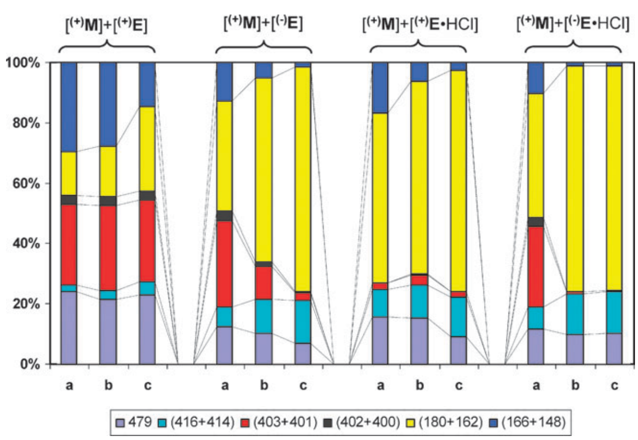

Fig. 2 Relative abundance of the fragment ions from CID (E_{lab} = 15 eV) of m/z 479 as a function of the relative concentrations of **E** and **M** in the electrosprayed solution ([**M**]/[**E**] = 0.5 (a); 1.0 (b); 2.0 (c)).

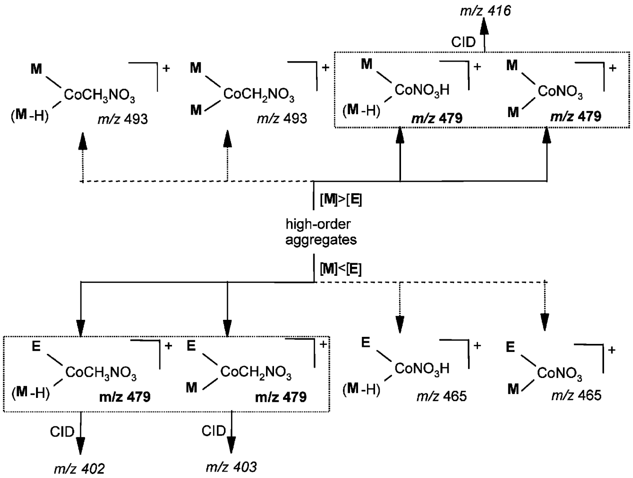

Scheme 1

On the grounds of the above evidence, it is proposed that the m/z 479 is generated in the ESI droplets by decomposition of higher-order aggregates of **M** and **E** around the $CoNO_3^+$ center, wherein extensive structural reorganization takes place before decomposition to the $[(\mathbf{M}-H)\mathbf{M}CoNO_3H]^+$, $[(\mathbf{M}-H)\mathbf{E}CoCH_3ONO_2]^+$, and $[\mathbf{ME}CoCH_2ONO_2]^+$ isomeric structures (Scheme 1). The nature of these higher-order aggregates and their tendency to undergo isomerization reactions markedly depend on the charge state, the relative concentration, and the configuration of the **M** and **E** molecules in the ESI droplets. This conclusion is reinforced by the isolation of an ion at m/z 493 among the ionic products from ESI of **M**–$Co(NO_3)_2$–CH_3OH solutions (Scheme 2). CID of this ion is characterized by the predominant formal loss of CH_2ONO_2 (to give m/z 417) and CH_3ONO_2 (to give m/z 416). This implies that both the $[\mathbf{M}_2CoCH_2ONO_2]^+$ and $[(\mathbf{M}-H)\mathbf{M}CoCH_3ONO_2]^+$ isomers contribute to the m/z 493 ion. Their formation necessarily requires respectively the formal methylene and methyl group transfer from **M** to the NO_3 moiety of higher-order $\mathbf{M}/CoNO_3^+$ aggregates during the ESI droplet evaporation. Work is in progress to identify and characterize these higher-order Co(II)/neurotransmitter aggregates involved in the fast stereoselective reactions of Schemes 1 and 2.

As a final remark, it should be pointed out that the present results have some connections with the mass spectrometric observation of different structures for the $[Co(III)(acac)_2/$diisopropyl-D-tartrate$]^+$ and $[Co(III)(acac)_2/$diisopropyl-L-tartrate$]^+$ complexes induced by the presence in the relevant solutions of the (*R*,*R*)-(+)- or (*S*,*S*)-(−)-hydrobenzoin "spectator" molecules which are actively and selectively involved in their formation.[24] It should be stressed that here, differently from the present case, the "spectator" molecules do not induce any reaction in the ESI-formed complexes, but simply influence the structural landscape of the $[Co(III)(acac)_2/tartrate]^+$ complexes by participating to their formation.

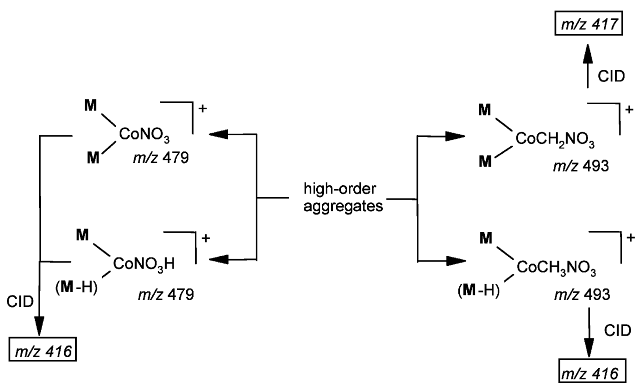

Scheme 2

Notes and references

‡ Operating conditions of the ESI source are as follows: ion spray voltage = +5.5 kV; sheath gas = 34 psi; nebulizer gas = 15 psi; focusing rod offset (IS) = +10 V; orifice plate = +35 V; capillary temperature = 210 °C. Methanolic solutions are infused *via* a syringe pump at a flow rate of 10 μL min^{-1}. CID experiments are performed in the following way: after isolation in the first quadrupole, precursor ions are allowed to go through the collision region, where their CID takes place. The survivor precursor and its product ions were accumulated in the linear trap (LIT) of the instrument (fill time of the trap = 20 ms; scan rate = 1000 u s^{-1}) to improve the signal-to-noise ratio and eventually detected. Operating conditions in CID experiments are: nominal pressure of nitrogen in collision chamber, 1.4×10^{-5} Torr; the CID collision energy (in eV; lab frame) is calculated from the difference in volts between IS and collision cell rod offset. The relative abundance of fragments results from area of peaks of the spectra acquired in profile mode. In each acquisition the final spectra are the average of about 70 scans, each consisting of two microscans. Standard deviation of relative ion abundances: ±10%.

1 A. Lapolla, D. Fedele, R. Seraglia and P. Traldi, *Mass Spectrom. Rev.*, 2006, **25**, 775.
2 A. B. Hummon, A. Amare and J. V. Sweedler, *Mass Spectrom. Rev.*, 2006, **25**, 77.
3 S. Schuchardt and A. Sickmann, *EXS*, 2007, **97**(Plant Systems Biology), 141.
4 Patriksson, E. Marklund and D. Van der Spoel, *Biochemistry*, 2007, **46**, 933.
5 M. F. Jarrold, *Annu. Rev. Phys. Chem.*, 2000, **51**, 179.
6 T. Wyttenbach, M. Witt and M. T. Bowers, *J. Am. Chem. Soc.*, 2000, **122**, 3458.
7 W. F. Smyth, S. McClean, C. J. Hack, V. N. Ramachandran, B. Doherty, C. Joyce, F. O'Donnell, T. J. Smyth, E. O'Kane and P. Brooks, *TrAC, Trends Anal. Chem.*, 2006, **25**, 572.
8 L. K. Zhang, D. Rempel, B. N. Pramanik and M. L. Gross, *Mass Spectrom. Rev.*, 2005, **24**, 286.
9 V. B. Di Marco and G. G. Bombi, *Mass Spectrom. Rev.*, 2006, **25**, 347.
10 R. Bakhtiar and C. E. C. A. Hop, *J. Phys. Org. Chem.*, 1999, **12**, 511.
11 H. M. Dion, L. K. Ackerman and H. H. Hill, *Talanta*, 2002, **57**, 1161.
12 S. D. Fuerstenal, *J. Mass Spectrom. Soc. Jpn.*, 2003, **51**, 50.
13 A. Bothner and G. Siuzdak, *ChemBioChem*, 2004, **5**, 258.
14 Y. Song, N. Talaty, W. A. Tao, Z. Pan and R. G. Cooks, *Chem. Commun.*, 2007, 61.
15 E. R. Wickremsinhe, G. Singh, B. L. Ackermann, T. A. Gillespie and A. K. Chaudhary, *Curr. Drug Metab.*, 2006, **7**, 913.
16 S. A. Hofstadler and K. A. Sannes-Lowery, *Methods Princ. Med. Chem.*, 2007, **36**(Mass Spectrometry in Medicinal Chemistry), 321.
17 S. C. Nanita, E. Sokol and R. G. Cooks, *J. Am. Soc. Mass Spectrom.*, 2007, **18**, 856.
18 P. Yang, R. Xu, S. C. Nanita and R. G. Cooks, *J. Am. Chem. Soc.*, 2006, **128**, 17074.
19 V. Znamenskiy, I. Marginean and A. Vertes, *J. Phys. Chem. A*, 2003, **107**, 7406.
20 P. Nemes, S. Goyal and A. Vertes, *Anal. Chem.*, 2008, **80**, 387.
21 C. L. Sherman and J. S. Brodbelt, *Anal. Chem.*, 2003, **75**, 1828.
22 J. E. Ham, B. Durham and J. R. Scott, *Rev. Sci. Instrum.*, 2005, **76**, 014101.
23 R. L. Grimm and J. L. Beauchamp, *J. Phys. Chem. B*, 2005, **109**, 8244.
24 T. T. Dang, S. F. Pedersen and J. A. Leary, *J. Am. Soc. Mass Spectrom.*, 1994, **5**, 452.